

Evolution of copper arsenate resistance for enhanced enargite bioleaching using the extreme thermoacidophile *Metallosphaera sedula*

Chenbing Ai^{1,2} · Samuel McCarthy² · Yuting Liang^{1,2} · Deepak Rudrappa² · Guanzhou Qiu¹ · Paul Blum²

Received: 12 May 2017 / Accepted: 26 July 2017 / Published online: 2 August 2017
© Society for Industrial Microbiology and Biotechnology 2017

Abstract Adaptive laboratory evolution (ALE) was employed to isolate arsenate and copper cross-resistant strains, from the copper-resistant *M. sedula* CuR1. The evolved strains, *M. sedula* ARS50-1 and *M. sedula* ARS50-2, contained 12 and 13 additional mutations, respectively, relative to *M. sedula* CuR1. Bioleaching capacity of a defined consortium (consisting of a naturally occurring strain and a genetically engineered copper sensitive strain) was increased by introduction of *M. sedula* ARS50-2, with 5.31 and 26.29% more copper recovered from enargite at a pulp density (PD) of 1 and 3% (w/v), respectively. *M. sedula* ARS50-2 arose as the predominant species and modulated the proportions of the other two strains after it had been introduced. Collectively, the higher Cu²⁺ resistance trait of *M. sedula* ARS50-2 resulted in a modulated microbial community structure, and consolidating enargite bioleaching especially at elevated PD.

Keywords Extreme thermoacidophile · Enargite bioleaching · *Metallosphaera sedula* · Arsenate resistance · Mutation

Electronic supplementary material The online version of this article (doi:10.1007/s10295-017-1973-5) contains supplementary material, which is available to authorized users.

✉ Paul Blum
pblum1@unl.edu

¹ School of Minerals Processing and Bioengineering, Central South University, Changsha 410083, People's Republic of China

² School of Biological Sciences, Beadle Center for Genetics, University of Nebraska-Lincoln, Room E234, 1901 Vine St., Lincoln, NE 68588-0666, USA

Introduction

Enargite (Cu₃AsS₄) is an important industrial copper ore that is common in porphyry ores and deep epithermal “high sulphidation” deposits and is associated with other major copper sulfides such as chalcopyrite (CuFeS₂) and chalcocite (Cu₂S) [16]. Recent studies showed that high recovery yields of copper can be rapidly obtained from enargite using hydrometallurgical processes, such as alkaline sodium sulfide leaching and pressure leaching [24, 29]. However, because of the large amount of sodium sulfide employed and special equipment requirements, these hydrometallurgical processes are not relevant for industrial application. In addition, there is currently no economical method to separate enargite from other copper sulfides, such as chalcopyrite, in industrial flotation processes when it occurs as an impurity [25]. Therefore, conventional pyrometallurgical technologies would inevitably cause environmental problems by emission of poisonous gas and dusts when processing arsenic-bearing copper sulfides.

Bioleaching offers an alternative to conventional technologies for enargite processing. Enargite is recalcitrant as its dissolution rate is very slow in acidic solution [30, 31]. *Acidithiobacillus ferrooxidans* is only able to bioleach 3% of the copper from enargite in 130 days at 25 °C [31]. However, bioleaching with extremely thermoacidophilic (optimal growth $T_m \geq 60$ °C, pH ≤ 3) archaea belonging to the phylum *Crenarchaeota* could be a promising alternative for the extraction of copper from enargite. This is predicated based on two process features: accelerated bioleaching rate and improved recovery yield resulting from the use of high incubation temperatures and minimization of surface passivation [27, 37]. However, both Cu²⁺ and As⁵⁺ ions accumulate in the leachate to high concentration during biomining of arsenic-bearing copper sulfide ores and

would challenge the survival and proliferation of extreme thermoacidophiles [41]. These organisms generally have a significantly lower minimal inhibitory concentration (MIC) of heavy metals/metalloids as compared with bioleaching mesophiles and moderate thermoacidophiles [23, 40]. Therefore, the availability of simultaneous resistance towards both copper and arsenic constitutes a desirable trait in extreme thermoacidophiles.

A variant of *M. sedula* with Cu^{2+} resistance up to 200 mM, named CuR1, was recently isolated in our laboratory through adaptive laboratory evolution (ALE) [18]. The supranormal cupric resistant trait of CuR1 indicates that it is eligible for the isolation of arsenate and copper cross-resistant strains through ALE. Previous studies on arsenic resistance have shown that the typical *ars* operons, such as *arsRCB* and *arsRCDAB*, are broadly distributed in biomining-relevant acidophilic bacteria [14, 15, 17]. However, none of these well-characterized arsenic resistance mechanisms were observed in the genomes of extremely thermoacidophilic archaea. In their absence, it is plausible that novel arsenic resistance mechanisms might exist in lithoautotrophic thermoacidophilic archaea.

Microbial consortia rather than pure cultures have been adopted to extract basic (copper, zinc) and precious (gold, nickel) metals from sulfide minerals in the biomining industry or at bench-scale studies [5, 9–11, 26]. Previous studies have shown that bioleaching consortia consisting of acidophiles belonging to different genera or species exhibited more dramatic bioleaching capacity due to higher Fe^{2+} /sulfur oxidation activity, and organic carbon source utilization relative to single pure cultures [22, 26]. In addition, succession of microbial community structure was observed when acclimating biomining consortia to high pulp density of chalcopyrite at bench-scale for two years or continuously processing gold-bearing arsenopyrite concentrate in stirred tanks at commercial scale for around two decades [5, 13, 26, 39]. Consistent with this idea, it has also been proposed that genetic mutation might enhance the growth and resistance of bioleaching species, therefore, altering the microbial community structure during bioleaching [26]. However, experimental data supporting this hypothesis are unavailable, which probably is ascribed to the lacking of quantitative techniques to differentiate these evolved strains from their closely related parental strains when they coexisted in the same consortium. If one of the strains had a unique genetic marker a quantitative PCR-based technique would be able to provide relevant data to support this hypothesis. The *M. sedula copA* mutant, a strain with a *pyrE* gene insertion in *copA* gene (Msed_0490), was the first genetically engineered bioleaching extremely thermoacidophile [18]. The copper resistance of the *M. sedula copA* mutant was reduced from 76 to 40 mM Cu^{2+} as compared with the parental

strain *M. sedula* DSM 5348 [18]. The copper-resistant *M. sedula* CuR1, a derivative of *M. sedula* DSM 5348 isolated through ALE, contained mutations in genome and showed increased copper resistance to 200 mM Cu^{2+} [19]. Therefore, either the *M. sedula* CuR1 or its derivatives isolated in this study can be adopted to construct a defined consortium together with the *M. sedula copA* mutant to simulate the adaptation to elevated pulp density of copper sulfide minerals (such as chalcopyrite and enargite).

The purpose of this study was to isolate and characterize novel *M. sedula* strains with cross-resistance to high levels of both arsenate and copper using an ALE process as described in our previous study [20]. Heterotrophic growth with 0.2% (w/v) tryptone as the sole energy substrate of the evolved strains under high concentrations of Cu^{2+} or As^{5+} was compared. Genetic changes were evaluated by genome resequencing. Additionally, the effects of introduction an isolated cross-resistant strain *M. sedula* ARS50-2 to a defined consortium (consisted of a naturally occurring *M. hakonensis* HO 1-1 and a genetically engineered *M. sedula copA* mutant) on the enargite bioleaching in batch cultures at different PD were studied. Finally, the successions of microbial community structure of these defined consortia were quantitatively analyzed by qPCR. The findings from this study provide insights into arsenate resistance mechanisms in arsenate and copper cross-resistant strains of *M. sedula*, and highlight the importance of genetic mutations on modulating the microbial community structure succession and its function during the bioleaching of copper sulfide ores.

Materials and methods

Archaeal strains and cultivation

Archaeal strains used in this study included *Metallosphaera sedula* DSM 5348T (wild type), the Cu^{2+} resistant strain *M. sedula* CuR1 [18], the Cu^{2+} sensitive strain *M. sedula copA* mutant [18], newly derived Cu^{2+} and As^{5+} cross-resistant strains *M. sedula* ARS50-1 and ARS50-2 [2], and *M. hakonensis* HO 1-1 [12]. Basal salts medium (BSM) [3] was adjusted to pH 2.0 using sulfuric acid, and supplemented with 0.2 or 0.1% (w/v) tryptone for heterotrophic growth of *M. sedula* strains and *M. hakonensis* HO 1-1, respectively, as described previously [18]. To test the Cu^{2+} and As^{5+} resistance capacities, CuSO_4 or KH_2AsO_4 (Sigma-Aldrich, USA) was added to the medium. The cultures were incubated at 75 °C in either glass screw-cap flasks with aeration in orbital baths or in glass screw-cap test tubes, which were placed in rotary drum agitator that was mounted in incubators as described previously [18].

Mineral components

Mineralogical components of enargite concentrate used in this study was identical with that described in a previous study: enargite (60%), pyrite (FeS_2) (30%), nowackiite ($\text{Cu}_6\text{Zn}_3\text{As}_4\text{S}_{12}$) (5%) and balance quartz, as indicated by X-ray diffraction (XRD) analyses [1]. The particle size of this concentrate was superfine, 84.1% of which was less than 30 μm in diameter. The main chemical composition of the concentrate was (w/w): 27.66% Cu, 9.59% As, 14.01% Fe, 39.75% S and 0.82% Zn.

Isolation of arsenate resistant *M. sedula* strains

The Cu^{2+} resistant *M. sedula* strain CuR1 was inoculated from a frozen permanent into 5 mL of medium for heterotrophic growth in glass screw-cap test tubes. Planktonic growth was monitored by the optical density at the wavelength of 540 nm. Mid-exponential phase cultures were repeatedly subcultured into fresh heterotrophic growth medium supplemented with a gradually increasing concentration of KH_2AsO_4 . After several weeks of passage, resistant cells grew heterotrophically in the presence of 50 mM As^{5+} in the medium and two clonal isolates were recovered using solid complex medium. Culture plates were prepared using basal salts medium (adjusted to pH 3.0 using sulfuric acid) mixed with 0.6% (w/v) gelrite (Kelco) and supplemented with 0.2% (w/v) tryptone. Plates were incubated at 75 °C for 5 days. The Cu^{2+} and As^{5+} cross-resistant capacities of two clonal isolates were tested and compared with their ancestral strain *M. sedula* DSM 5348T (wild type) and parental strain *M. sedula* CuR1, respectively.

Genome resequencing and nucleotide sequence accession numbers

Genomic DNA isolation, sequencing and sequence assembly were carried out as described previously [2]. The nucleotide sequences have been deposited with GenBank under accession no. CP012172 and CP012173 for re-sequenced *M. sedula* ARS50-1 and *M. sedula* ARS50-2, respectively [2].

Bioleaching experiments

Prior to inoculation with cells, 1 and 3% (w/v) enargite concentrate were, respectively, added to 50 mL BSM medium adjusted to pH 2.0 with sulfuric acid in 250 mL screw-cap glass flasks and incubated at 75 °C with agitation (175 rpm) for 24 h to wash out the residual floatation reagents in the minerals. The enargite residue was collected by centrifugation at 3000 rpm for 5 min, suspended and transferred into 250 mL flasks containing 50 mL of fresh BSM medium (pH 2.0) supplemented with 0.05% (w/v) tryptone. A total

number of 1.8×10^9 cells of either pure *Metallosphaera* strains or mixed *Metallosphaera* spp. cultures (consortia) were then added to the flasks.

Two consortia were constructed for enargite bioleaching. Consortium A consisted of *M. sedula copA* mutant and *M. hakonensis* HO 1-1, while consortium B contained *M. sedula copA* mutant, *M. hakonensis* HO 1-1 and *M. sedula* ARS50-2. The copper sensitive *M. sedula copA* mutant was used to construct the defined consortia instead of the ancestral wild type *M. sedula* because it contains a *pyrE* gene insertion in *copA* gene (Msed_0490). This unique genetic marker can be screened for and quantitatively measured by qPCR. *M. hakonensis* HO 1-1 is an extremely thermoacidophile with high sulfur oxidation capacity and has the potential for bioleaching refractory chalcopyrite [6, 32]. *M. hakonensis* HO 1-1 was included in consortium to consolidate the sulfur oxidation capacity. *M. sedula* ARS50-2 rather than *M. sedula* ARS50-1 was adopted to construct consortium B because it showed a slightly higher growth rate when grown heterotrophically in the presence of 140 mM Cu^{2+} or 75 mM As^{5+} . The adaptive evolution, genetic differences and metal/metalloid resistance capacities of the cross-resistant *M. sedula* ARS50-2 and the copper sensitive *M. sedula copA* mutant were compared (Fig. S1). All experiments were conducted in duplicates and abiotic controls for each pulp density were included under the same conditions. All samples were incubated at 75 °C in glass screw-cap flasks with agitation in orbital baths. Evaporated water was compensated daily by addition of distilled water based on weight loss. One milliliter supernatant samples were taken at 3 days interval for analysis of the ionic concentrations and the planktonic cell number.

Analytical methods

Planktonic cell numbers were counted using a Thoma counting chamber under light microscope. The pH of the leachate was measured using a pH meter (Fisher Scientific, Model AB30). The Eh value of leachate was determined using a platinum electrode with an Ag/AgCl reference electrode (American Marine Pinpoint ORP Monitor). The concentration of $\text{Fe}^{2+}/\text{Fe}^{3+}$ was quantified using the Ferrozine assay [34]. The concentration of Cu^{2+} was determined spectrophotometrically with diethyldithiocarbamate (DDTC) at a wavelength of 440 nm [38]. The total concentrations of extracellular arsenic ions were quantified by inductively coupled plasma mass spectrometry (ICP-MS) as described previously [28]. Briefly, culture samples were clarified by centrifugation. Samples of the resulting supernatants were analyzed by ICP-MS using an Agilent ICP-MS 7500cx. A certified arsenate reference standard was used for sample normalization. All reported values are averages from duplicate samples.

Microbial community structure analysis by qPCR

Leachate samples (4 mL) were centrifuged at 2500 rpm for 20 s to remove solid particulates. The supernatants were then transferred to separate tubes and centrifuged at 10,000g for 5 min to pellet the cells. Genomic DNA was prepared from the pellets using a Wizard[®] Genomic DNA Purification Kit (Promega). Strain-specific PCR primer pairs for qPCR were designed (Table 1) and validated by PCR (one cycle of 95 °C for 5 min, and then 31 cycles of 95 °C for 15 s, 64 °C for 30 s, and 72 °C for 30 s) and agarose gel electrophoresis. The qPCR was performed using an iCycler iQ Real-time PCR detection system (Bio-Rad Laboratories, Inc.). Procedures for the detection of the specificity of primers and for qPCR were as described [42]. The reaction mixture contained 12.5 µl SYBR[®] Green Real-Time PCR Master Mix (Toyobo Co., Ltd., Osaka, Japan) which contains SYBR Green I dye, Taq DNA polymerase, dNTP and MgCl₂; and 1 µl of 10 µM solution of sense/anti-sense primer, 0.2 µl or 1 µl of genomic DNA. H₂O was added into the reaction mixture to a final volume of 25 µl. The qPCR program was identical with the aforementioned PCR program except for the cycle number increased to 40. After the completion of each run, melting curves for amplicons were measured by raising the temperature 0.5 °C from 55 to 95 °C while monitoring fluorescence. The cell abundance of *M. sedula* ARS50-2 in consortium B was calculated by subtracting the cell abundance of *M. sedula copA* mutant from the cell abundance of total *M. sedula* strains.

Results and discussion

Phenotypic response to copper and arsenate

The heterotrophic growth of wild type, *M. sedula* DSM 5348 (WT-Mse), the copper-resistant strain CuR1, and the newly isolated copper and arsenate resistant strains *M. sedula* ARS50-1 and *M. sedula* ARS50-2 were examined in the presence of 140 mM Cu²⁺ or 75 mM As⁵⁺ (Fig. 1). All strains grew to stationary phase in the absence of added

copper and arsenate in approximately 2.5 days (Fig. 1a). *M. sedula* CuR1, *M. sedula* ARS50-1 and *M. sedula* ARS50-2 grew in the presence of 140 mM Cu²⁺ with no apparent growth lag (Fig. 1b). This indicated that the high copper resistance of *M. sedula* ARS50-1 and *M. sedula* ARS50-2 was inherited from their parental strain, CuR1. Of the strains tested, only *M. sedula* ARS50-1 and *M. sedula* ARS50-2 grew well in the presence of 75 mM As⁵⁺ (Fig. 1c). Under identical conditions, no growth was observed for either the wild type or CuR1. The MIC for As⁵⁺ for CuR1 was found to be 30 mM when grown in flasks. This is the first report on the isolation of high level arsenic and copper cross-resistance for an extremely thermoacidophilic member of the archaea. Importantly, this trait was heritable. *M. sedula* ARS50-1 and *M. sedula* ARS50-2 retained the ability to grow well in the presence of 75 mM As⁵⁺ despite passaging them three times in medium without As⁵⁺. This finding also excluded the possibility that arsenate resistance was stress-induced form of metalloid resistance. Finally, both the Fe²⁺ and sulfur oxidation capacities of *M. sedula* ARS50-1 and *M. sedula* ARS50-2 remained almost identical with that of the wild type *M. sedula* and the parental strain CuR1. This might indicate that the genes involved in Fe²⁺ and sulfur oxidation pathways were not affected by mutations during the adaptive laboratory evolution process.

Genome resequencing of cross-resistant *M. sedula* strains

The significant phenotypic difference between CuR1 and its arsenate resistant derivatives, *M. sedula* ARS50-1 and ARS50-2, under high concentration of As⁵⁺ might have arisen due to mutation(s) accumulated during the adaptive process and their identities might provide insights into the mechanism of arsenate resistance. Genome resequencing resulted in a sequence depth of 240-fold for both *M. sedula* ARS50-1 and *M. sedula* ARS50-2 (Table 2). Genome resequencing data showed that *M. sedula* ARS50-1 and *M. sedula* ARS50-2 gained 12 and 13 mutations, respectively, with five shared mutations in both strains during the adaptive process. This period consisted of 28

Table 1 Strain specific qPCR primer pairs for *Metallosphaera* spp. based on the *copA* gene

Target strain	Primer name	Sequence (5' to 3')	Amplicon length (bp)
<i>M. hakonensis</i> HO1-1	Mha-F	ATGCGGTCGTAGTCAAATCT	185
	Mha-R	TGCTCTCGTGACGTATACGCGT	
<i>M. sedula copA</i> mutant	CopA-F	GGACTCGAGGAAATTGAGGGTT	167
	CopA-R	CTTAACCTGGGTAAGGAGAAAGT	
<i>M. sedula</i> spp.	Mse-F	GTTTACGGGAAGGTAGATCAACAT	198
	Mse-R	AATGATTACCCCGAATCTCC	

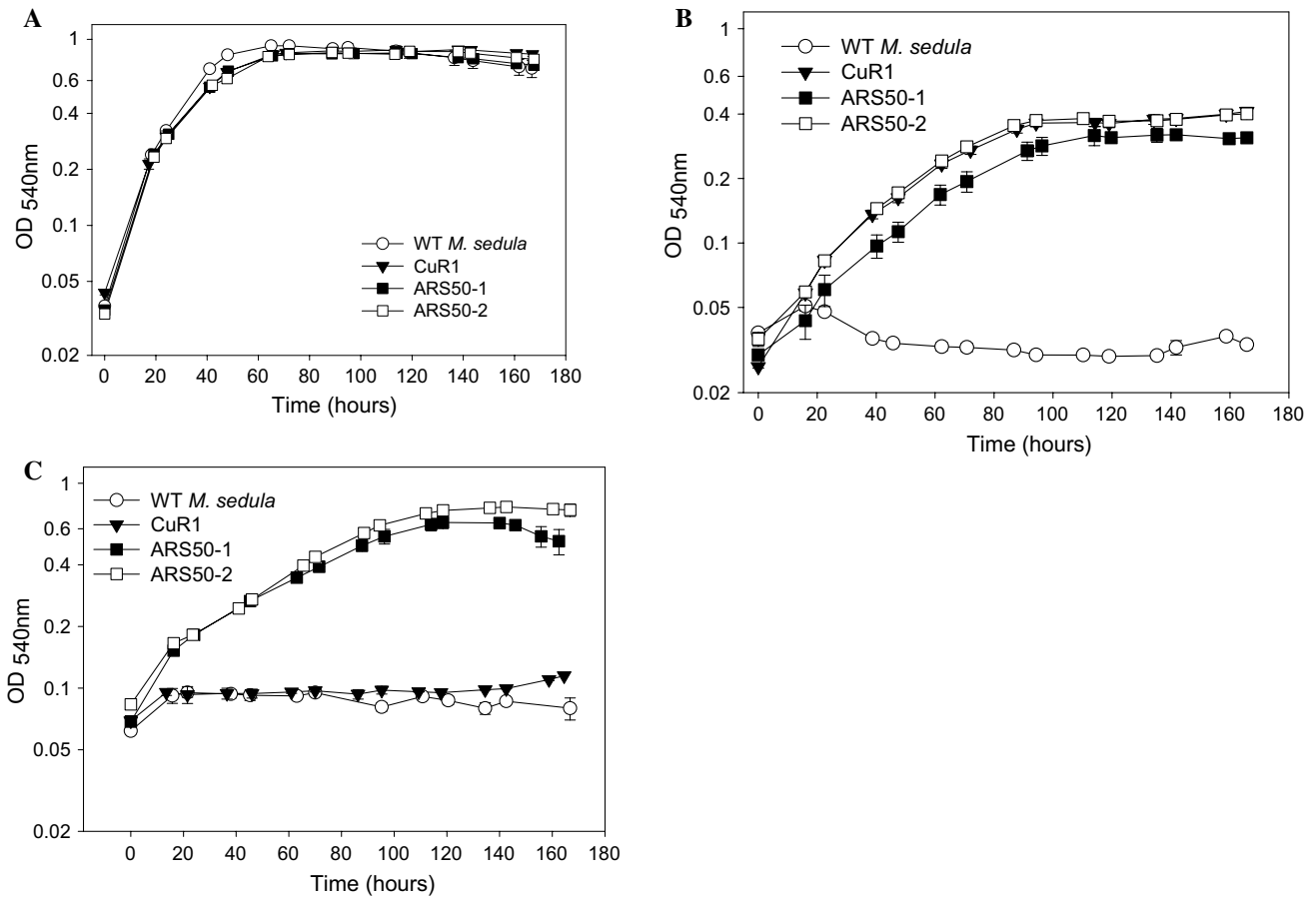


Fig. 1 Heterotrophic growth curves of different *M. sedula* strains in the absence of extra $\text{Cu}^{2+}/\text{As}^{5+}$ (a), in the presence of 140 mM Cu^{2+} (b) or 75 mM As^{5+} (c). WT-Mse (*M. sedula* DSM 5348T), CuR1 (*M. sedula* CuR1), ARS50-1 (*M. sedula* ARS50-1), ARS50-2 (*M. sedula* ARS50-2)

Table 2 Summary of sequencing coverage and mutations

Strain name	Depth of coverage by Illumina reads (fold)	Substitutions in ORFs	Substitutions in intergenic regions	References
Wild type <i>M. sedula</i>	1050	24	3	[19]
<i>M. sedula</i> CuR1	821	17	3	[19]
<i>M. sedula</i> ARS50-1	240	6	6	This study
<i>M. sedula</i> ARS50-2	248	7	6	This study

generations (cell divisions) occurring through nine consecutive culture passages. This resulted in a mutation rate of $(2.20 \pm 0.11) \times 10^{-7}$ mutations per cell division. This rate was comparable to the mutation rate for the CuR1 as described previously [19].

Both genomes had mutations in both coding regions and intergenic regions relative to their parental strain, CuR1 (Table 2). Only insertions and non-synonymous mutations evident in coding regions were further considered because these were most likely to alter gene functions. A tabulated summary of these mutations with detailed information including mutation position in the genome, gene

annotation, mutation type, gene/protein length and its proximity to identified domains is presented in Table 3. Two non-synonymous mutations were observed in Msed_0837, a pseudogene, in the genome of *M. sedula* ARS50-2, which might encode a transposase as indicated by BLAST analysis. A non-synonymous mutation led to the change of Gly163 to Glu163 in Msed_1139, which located in the conserved domain CsaX_III_U. Currently, the physiological role of Msed_1139 remains unknown. A non-synonymous mutation changing Asp31 to Asn31 (acidic to neutral) was mapped to the extracellular region of Msed_1340, which encoded a small membrane protein containing two transmembrane

Table 3 Summary of mutations in *M. sedula* ARS50-1 and *M. sedula* ARS50-2 genome as compared with parental strain CuR1

Genome coordinate	Substitution and/or description	Msed ORF	Gene function	Mutation location	Domain affected	Strain name
766, 422	T → C, non-synonymous (Leu → Ser)	0837	Pseudogene	nt 189/1218; aa 63/271		ARS50-2
766, 447	A → G,	0837	Pseudogene	nt 214/1218; aa 72/271		ARS50-2
1, 076, 708	C → T, non-synonymous (Gly → Glu)	1139	Type I-A CRISPR-associated protein CsaX	nt 488/1029; aa 163/342	CsaX_III-U	ARS50-1 ARS50-2
1, 315, 693	G → A, non-synonymous (Asp → Asn)	1340	Hypothetical	nt 91/240; aa 31/79		ARS50-1 ARS50-2
1, 377, 017	C → T, non-synonymous (Cys → Tyr)	1407	Hypothetical	nt 29/300; aa 10/99		ARS50-1 ARS50-2
1, 793, 232	1-nt insertion of T, truncate the ORF by 15 nt	1846	FkbM family methyltransferase	nt 870/912		ARS50-1 ARS50-2
1, 838, 278	T → C, non-synonymous (Asn → Asp)	1892	Hypothetical	nt 67/1137; aa 23/378		ARS50-1
1, 985, 172	A → C, non-synonymous (His → Pro)	2066	Uncharacterized membrane-associated protein	nt 248/600; aa 83/199	DedA domain	ARS50-1
1, 985, 139	1-nt insertion of T, truncate ORF to 228 nt	2066	Uncharacterized membrane-associated protein	nt 213/600	DedA domain, curtail ORF from 199 aa to 75 aa	ARS50-2

helices, but had no known function or conserved domains. This mutation might change the physiological function of Msed_1340 to some extent. Msed_1407, which encoded a small cytoplasmic protein with the physiological function unknown, underwent a non-synonymous mutation in both strains consisting of a change from Cys10 to Tyr10 at the N-terminal. Msed_1846, which encoded an S-adenosylmethionine (SAM) dependent FkbM family methyltransferase in *M. sedula*, underwent a 1-nt insertion that truncated the gene sequence by 15 nucleotides. Consequently, the fragment constituted by the 13 amino acid residues at the C-terminal was substituted by another 8 amino acid residues. The effects of this C-terminal event on the physiological function of Msed_1846 was unknown, although it lied outside the conserved domain. The FkbM methyltransferase from *Streptomyces tacrolimus* was involved in methylating the C-31 hydroxyl group of 31-O-demethyl-FK506 and FK520 to enable synthesis of macrocyclic polyketides [21]. However, as the genes needed for biosynthesis of the macrolactone ring of FK506 were absent in the genome of *M. sedula* [4], it was unlikely that Msed_1846 involved in polyketide synthesis. The SAM-dependent methyltransferase involved in the methylation of various molecules, including proteins, DNA and secondary metabolites [35]. Whether the Msed_1846 was relevant to arsenate resistance remained to be identified. The hypothetical protein Msed_1892 contained a non-synonymous change of Asn23 to Asp23. This protein contained a LanC-like superfamily domain. However, the mutation was outside of this region. As the natural amino

acid was not conserved among homologs in other extremely thermoacidophilic species, this mutation might not affect the physiological role of Msed_1892. The uncharacterized membrane-associated protein Msed_2066 contained a non-synonymous change from His83 to Pro83 in the genome of *M. sedula* ARS50-1. Since this amino acid residue was not highly conserved among the homologs of Msed_2066 from extremely thermoacidophiles, this mutation might not change the physiological function. This gene contained a conserved DedA domain and recent studies showed that DedA membrane proteins from *E. coli* involved in cell division, membrane homeostasis, pH/PMF homeostasis and temperature sensitivity [8]. In the genome of *M. sedula* ARS50-2 there was a 1 nt insertion of T that truncated Msed_2066 from 600 nt to 228 nt. This mutation probably inactivated the gene. However, no significant difference in arsenate resistance was observed between *M. sedula* ARS50-1 and *M. sedula* ARS50-2 apparently excluding a role for Msed_2066 in arsenate resistance (Fig. 1c).

Enargite concentrate bioleaching by pure culture of *Metallosphaera* spp

Bioleaching capacities of each pure culture of the *Metallosphaera* strains were evaluated by processing enargite concentrate at PD of 1% (w/v) (Fig. 2). Different bioleaching behaviors were observed between *M. hakonensis* HO 1-1 and these two *M. sedula* strains.

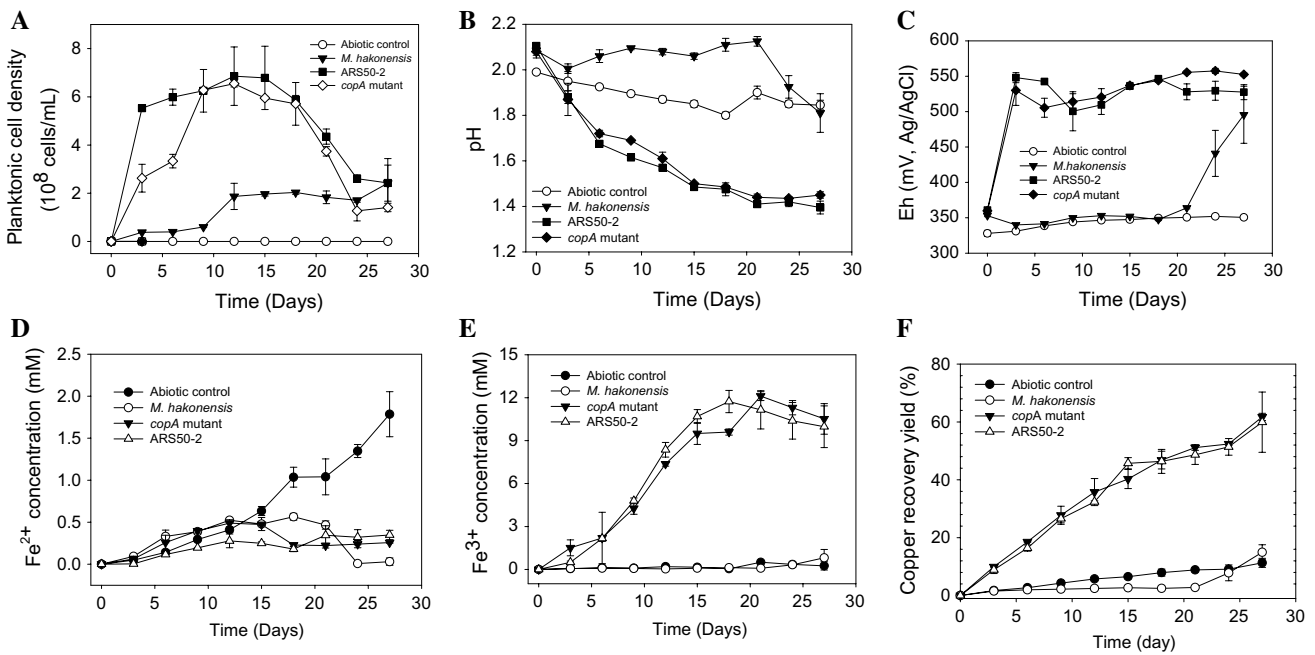
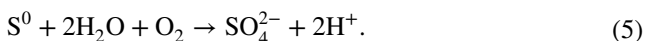
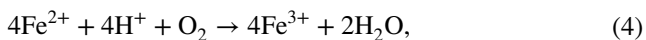
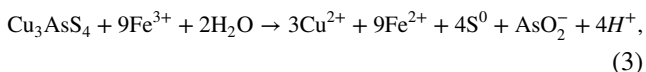
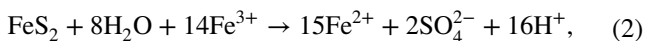
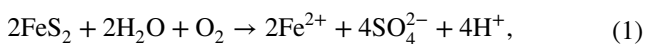


Fig. 2 Changes of planktonic cell number (a), pH value (b), Eh values (c), Fe^{2+} ion (d), Fe^{3+} ion (e), and copper recovery yield (f) of enargite bioleached by pure cultures of *Metallosphaera* spp. at PD of 1% (w/v)

The planktonic cell numbers of the *M. sedula copA* mutant and *M. sedula* ARS50-2 increased rapidly after inoculation and reached the plateau (around 6×10^8 cells/mL) at the 9th day followed by a decrease after the 15th day (Fig. 2a). However, the cell density of *M. hakonensis* HO 1-1 in leachate remained at low level (around 4×10^7 cells/mL) during the first 9 days. After this period its cell density increased to 2×10^8 cells/mL and remained at this level throughout the duration of the experiment (Fig. 2a). The survival of these extremely thermoacidophiles indicated that they can effectively utilize the sulfur and/or ferrous iron dissolved from enargite concentrate for growth [Eqs. (1)–(5) [33, 36]. The pH values of the leachate of *M. sedula copA* mutant and *M. sedula* ARS50-2 decreased steadily after inoculation (Fig. 2b). This indicated that sulfur was efficiently mobilized from enargite and pyrite, and was further oxidized to sulfate and generated protons by these extreme thermoacidophiles (Fig. 2b) [Eqs. (3) and (5)]. However, the pH of the leachate of *M. hakonensis* HO1-1 remained largely unchanged before the 21st day, thereafter it decreased. Only a slight decrease of pH was observed for the abiotic control (Fig. 2b). The Eh of the leachate of abiotic control remained around 340 mV (using an Ag/AgCl electrode as a reference) (Fig. 2c). The Eh of *M. hakonensis* HO 1-1 remained around 340 mV till the 21st day, then increased up to terminal value of 482 mV. On the contrary, the Eh of both *M. sedula copA* mutant and *M. sedula* ARS50-2 increased rapidly to around 540 mV and then remained largely unchanged (Fig. 2c). The concentration of Fe^{2+} in leachate remained

at low level throughout the bioleaching process in the presence of extremely thermoacidophile (Fig. 2d). The Fe^{3+} concentration in leachate of *M. sedula* ARS50-2 and *M. sedula copA* mutant increased drastically since the 3rd day after inoculation and reached a plateau on the 18th and 21st day, respectively (Fig. 2e). This indicated that *M. sedula* strains can effectively dissolve pyrite, the only iron-bearing mineral in the enargite concentrate, to obtain the energy for survival through ferrous iron oxidation and generate the ferric iron for the enargite and pyrite leach [Eqs. (2) and (3)]. On the contrary, the Fe^{3+} concentrations of *M. hakonensis* HO1-1 remained at low level (almost 0 mM before the 24th day), which was comparable with that in the abiotic control (Fig. 2e). This should be attributed to the deficiency of Fe^{2+} oxidation ability for *M. hakonensis* HO1-1. This assumption was validated by comparison its ferrous iron oxidation capacity with the other two *M. sedula* strains with the ferrous iron as the sole energy substrate (Fig. S2). The inability of *M. hakonensis* HO1-1 to oxidize ferrous iron to Fe^{3+} would lead to the unavailability of sufficient ferrous and sulfur, the energy substrates for the cellular metabolism, that originally released from enargite and pyrite [(Eqs. (1)–(3)]. Therefore, fewer planktonic cells were sustained and an accordingly higher pH value of leachate together with much lower Eh was observed during the bioleaching by *M. hakonensis* HO1-1. Consistent with the concentration of Fe^{3+} in leachate, moderately high copper recovery yields were achieved by pure cultures of *M. sedula copA* mutant (61.73%) and *M. sedula* ARS50-2 (59.93%) (Fig. 2f). Only 11.30% and

14.95% copper was recovered from enargite concentrate for the abiotic control and *M. hakonensis* HO1-1, respectively.



Enargite concentrate bioleaching by consortia

By comparison of the bioleaching behaviors between consortium A (consisted of *M. sedula copA* mutant and *M. hakonensis* HO 1-1) and consortium B (consisted of *M. sedula copA* mutant, *M. hakonensis* HO 1-1 and *M. sedula* ARS50-2) at the PD of 1 and 3% (w/v), it was obvious that introducing *M. sedula* ARS50-2 into consortium A improved the enargite concentrate bioleaching, especially at the PD of 3% (w/v) (Fig. 3).

The planktonic cell numbers of consortium A and consortium B increased dramatically to their respective plateaus 15 days after the initiation of bioleaching, without a lag phase was observed (Fig. 3a). The planktonic cell number of consortium B was always higher than that of consortium A

at each pulp density, which might indicate that more energy substrates, such as ferrous iron and sulfur, were mobilized from the enargite and pyrite for the proliferation of the cultures in the presence of *M. sedula* ARS50-2. Significant increase in the planktonic cell number of each consortium was observed at the PD 3% (w/v) on the 21st and 24th day as compared to that at the PD of 1%.

The pH values of leachate of both consortia significantly decreased compared with the abiotic control starting on the 3rd day after inoculation (Fig. 3b). The pH value of consortium B was slightly lower than that of consortium A throughout the experiment at the PD of 1% (w/v) (Fig. 3b). This observation might indicate that the sulfur oxidation activity of consortium B was only slightly higher than that of the consortium A at this pulp density. It was worth to mention that the pH values of both consortia were much lower than that of each of these pure cultures from the 9th day after the initiation of the bioleaching at PD of 1% (w/v) by inoculating identical amount of cells, either pure culture or mixed cultures (Fig. S3a). This indicated that the *M. hakonensis* HO 1-1 improved the sulfur oxidation activities of the consortia when it coexisted with *M. sedula copA* and/or *M. sedula* ARS 50-2. Therefore, the defined consortia constructed in this study were robust regarding on the sulfur oxidation capacity in spite of few extremely thermoacidophilic strains adopted. The pH of consortium A at the PD of 3% (w/v) remained much higher than that at the PD of 1% (w/v). This indicated that sulfur oxidation

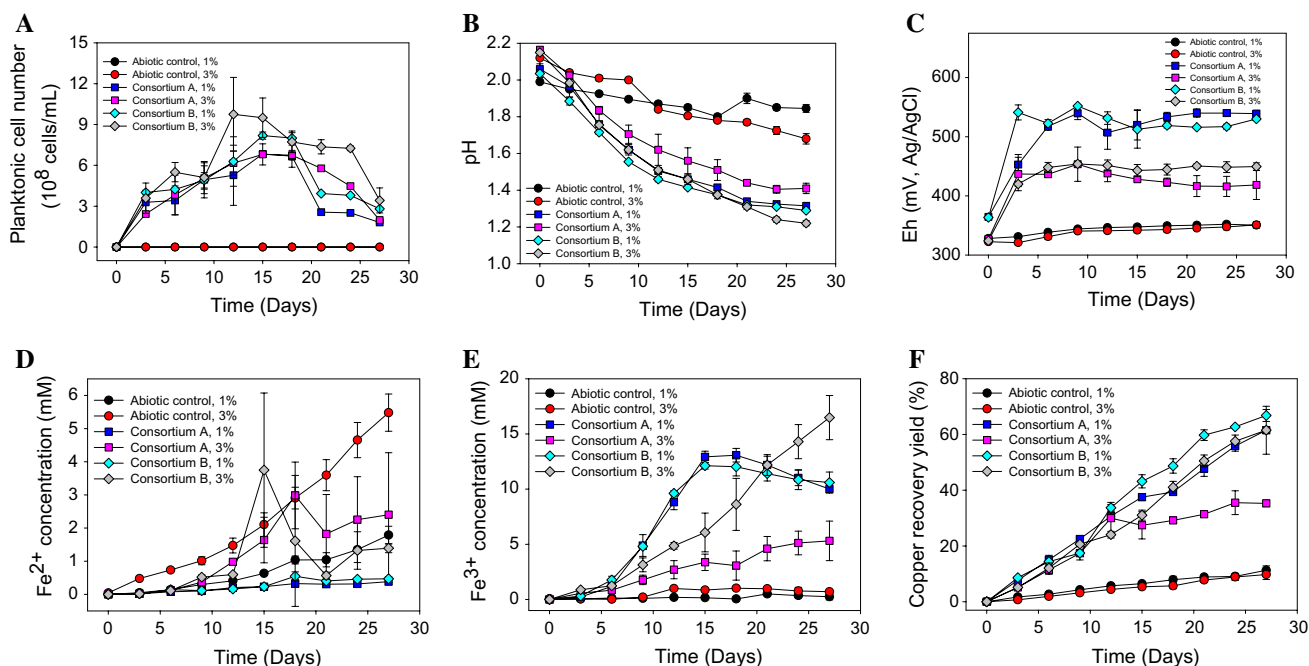


Fig. 3 Changes of planktonic cell number (a), pH value (b), Eh values (c), Fe²⁺ ion (d), Fe³⁺ ion (e), and copper recovery yield (f) of enargite bioleached by consortia consisted of *Metallosphaera* spp. at PD of 1 and 3% (w/v)

activity of consortium A was inhibited by the increased pulp density of minerals. However, the pH of consortium B at 3% (w/v) PD was much lower than that of consortium A; this difference continued to increase over time. This indicated that consortium B probably had a higher sulfur oxidation capacity.

The Eh of the leachate of consortium A and consortium B were very similar, and remained almost unchanged at around 540 mV (vs. Ag/AgCl) after the 6th day at the PD of 1% (w/v) (Fig. 3c). Both the leachate of consortium A and consortium B had much lower Eh at PD of 3% (w/v). The Eh of consortium B was obviously higher than that of consortium A after the 9th day at PD of 3% (w/v). This observation indicated that the ferrous iron oxidation capacity of consortium A, which only contained a metal sensitive *Fe*²⁺ oxidizer *M. sedula copA* mutant, was significantly inhibited; however, a compromised inhibitory effect was observed for consortium B, which contained another *Fe*²⁺ oxidizer, the cross-resistant *M. sedula* ARS50-2, as compared with consortium A. This assumption was further confirmed by the increase of ferrous iron and the decrease of ferric iron accompanied with the elevated PD (Fig. 3d, e). At the PD of 3%, the concentration of *Fe*²⁺ in both consortia remained much higher than that of each consortium at the PD of 1% (w/v) (Fig. 3d). The concentration of *Fe*²⁺ in leachate of consortium A and consortium B increased slightly in the first 12 days, and peaked at 18th and 15th day, respectively, then started to decrease (Fig. 3d). The concentration of *Fe*²⁺ in consortium A was higher than that of consortium B after the 18th day. The concentration of *Fe*³⁺ in leachate of consortium A and consortium B at PD of 1% (w/v) increased drastically after the 3rd day, peaked at the 15th day, and started to decrease gradually after the 18th day (Fig. 3e). The concentration of *Fe*³⁺ of consortium B increased greatly since the 6th day, and reached 16.48 mM at the 27th day at the PD of 3% (w/v) (Fig. 3e); while the concentration of *Fe*³⁺ in consortium A only increased slightly after inoculation, and reached 5.31 mM at the end of the bioleaching (Fig. 3e). These data indicate that consortium B had much higher *Fe*²⁺ oxidation capacity as compared with consortium A at the PD of 3%.

Consistent with the comparable concentration of *Fe*³⁺ generated in leachate by each consortium, moderately high copper recovery yields were achieved from enargite concentrate by consortium A (61.52%) and consortium B (66.83%) at the PD of 1% (w/v), respectively, after 27 days of bioleaching (Fig. 3f). Compared with the copper recovery yield achieved by each of these ferrous iron oxidizing *M. sedula* strains, only the consortium B had a slightly higher copper recovery yield at the PD of 1%(w/v) (Fig. S3b). Nevertheless, this indicates that the sulfur oxidizing *M. hakonensis* HO 1-1 has the potential to consolidate the bioleaching process together with these *M. sedula* strains. With the increase of PD to 3% (w/v), moderately high

copper recovery yield (61.57%) was achieved by consortium B; however, only 35.28% copper was recovered by consortium A.

Previous study has shown that mineral particles, especially at elevated pulp density, impose mechanical damage to bioleaching acidophile via attrition in stirred reactors [7]. The mechanical damage might contribute to the decreased copper recovery yield of each consortium at the PD of 3% (w/v) as compared with that at the PD of 1%(w/v) in this study. However, the mechanical damage alone cannot explain why there were significant differences between consortium A and consortium B during bioleaching at PD of 3% regarding on the planktonic cell number, pH value, Eh, *Fe*²⁺/*Fe*³⁺ concentration and copper recovery yield (Fig. 3a–f). Instead, these differences were probably correlated with the *Cu*²⁺ concentration in leachate (Fig. 4). The *Cu*²⁺ ion in leachate of consortium A increased steadily to 39.17 mM in the first 12 days, and remained almost unchanged until the 21st day, and then increased slightly to 46 mM till the end of bioleaching at the PD of 3% (w/v). The *Cu*²⁺ ion that mobilized from enargite concentrate accumulated to inhibitory concentration to *M. sedula copA* mutant (with a MIC of 40 mM), the only ferrous iron oxidizer in consortium A, and therefore inhibited the ferrous oxidation capacity of this consortium since the 12th day as reflected by the increased *Fe*²⁺ concentration together with the low *Fe*³⁺ concentration and Eh since the 12th day (Fig. 3c–e) [18]. It was undoubtedly that the activity of *M. sedula copA* mutant in consortium B was inhibited further at the PD of 3% (w/v) because much higher concentration of *Cu*²⁺ ion was accumulated in leachate after the 15th day (Fig. 4). Since the other ferrous iron oxidizer, *M. sedula* ARS50-2, in consortium B has a much higher MIC for *Cu*²⁺ ion (more than 140 mM), only a compromised inhibitory effect was observed in consortium B during the bioleaching at the PD of 3% (w/v) (Fig. 3c–e).

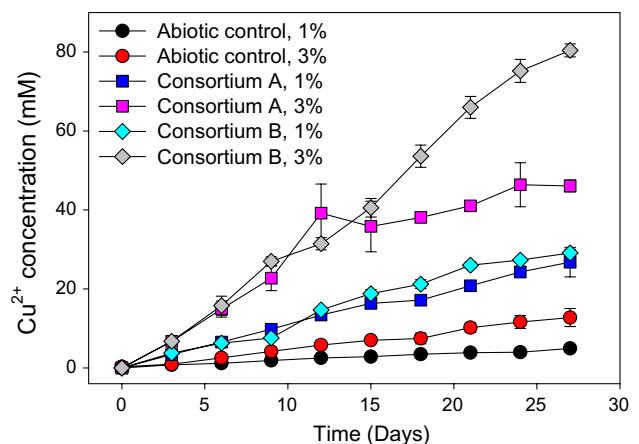


Fig. 4 Changes of *Cu*²⁺ concentration in leachate during enargite bioleaching at PD of 1 and 3% (w/v)

The arsenic ions in leachate of each consortium at the 12th and 21st day at each PD were analyzed to ascertain if it also affected the bioleaching processes at elevated PD (Fig. S4). The arsenic ions in leachate of consortium A and consortium B at the PD of 1 and 3% (w/v) was low at the 12th and 21st day, which was not proportionated to the concentration of Cu²⁺ during enargite bioleaching. A similar observation was showed in a previous study during enargite bioleaching by extremely thermoacidophilic *Acidianus brierleyi*, ascribing to the formation of scorodite (FeAsO₄·2H₂O) [37]. Therefore, the low arsenic concentration in leachate in the presence of extremely thermoacidophiles in this study probably also resulted from the precipitation of scorodite. The arsenic concentration was much less than the MIC of these *M. sedula* strain (30 mM for *M. sedula*

copA mutant and 75 mM for *M. sedula* ARS50-2). Therefore, the arsenic ions in leachate did not affect the activity of both consortia at each PD.

Microbial community structure analysis by qPCR

The succession of microbial community structure during the bioleaching of enargite at PD of 1 and 3% (w/v) was quantitatively analyzed by qPCR based on the strain-specific primer pairs (Fig. S5). By comparison the microbial community succession between consortium A and consortium B at the PD of 1 and 3% (w/v), it was obvious that introducing *M. sedula* ARS50-2 into consortium A decreased the viability of *M. sedula copA* mutant and increased the viability of *M. hakonensis* HO1-1 in consortium (Fig. 5).

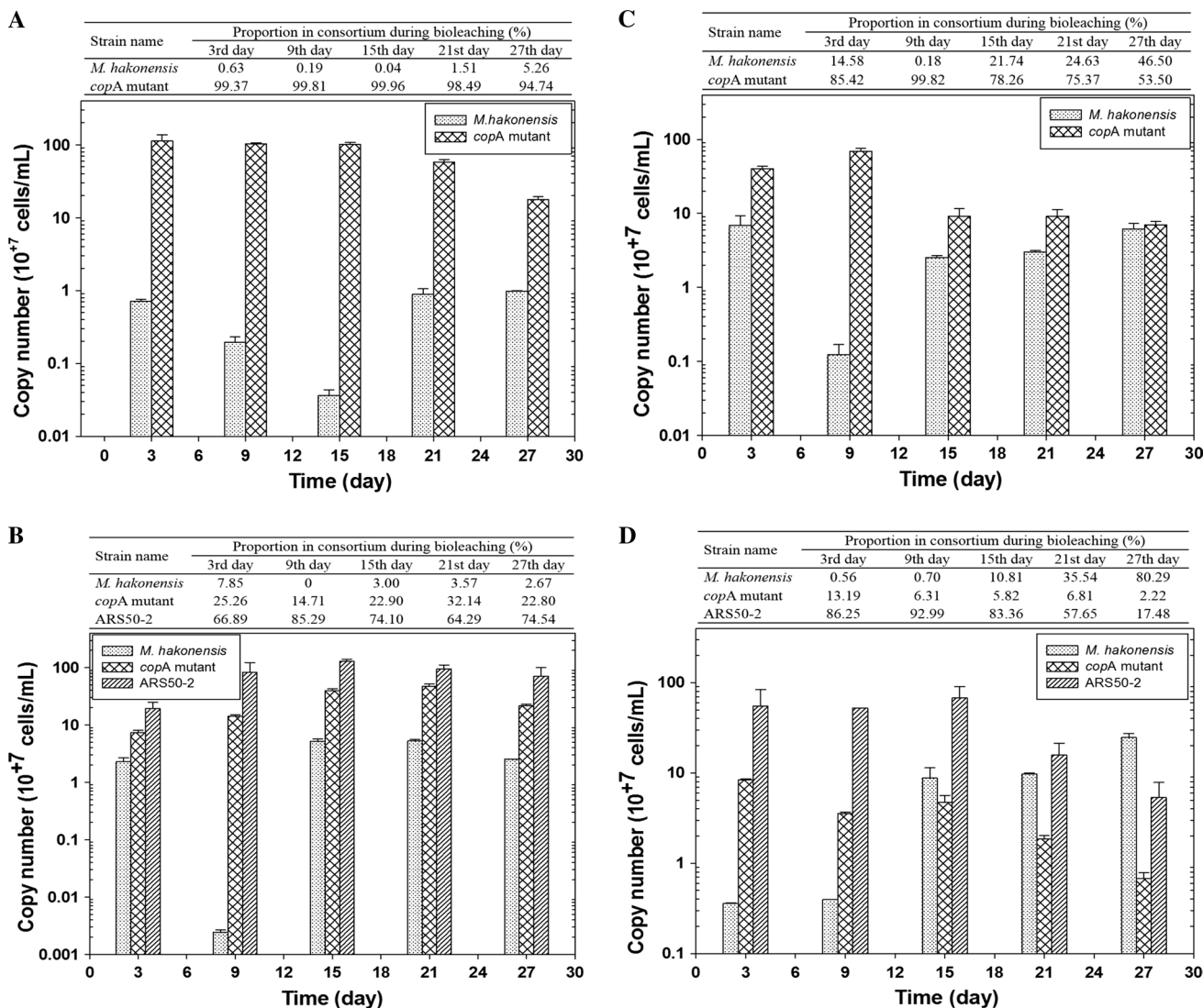


Fig. 5 Microbial community succession during the bioleaching of enargite with extremely thermoacidophilic consortia **a** consortium A at PD 1% (w/v); **b** consortium B at PD 1% (w/v); **c** consortium A at PD 3% (w/v); **d** consortium B at PD 3% (w/v)

M. sedula copA mutant was the predominant species in consortium A during the bioleaching of 1% (w/v) enargite (Fig. 5a), which was consistent with the observations that the arsenic ions and Cu^{2+} in leachate were not inhibitive to it (Fig. 4 and Fig. S4). *M. hakonensis* HO 1-1 was found with low proportion in leachate throughout the bioleaching process, possibly due to its deficiency in utilizing Fe^{2+} to obtain the energy for cell growth. *M. sedula* ARS50-2 substituted *M. sedula copA* mutant as the major species in consortium B at PD of 1% (w/v) (Fig. 5b). The cell abundance of *M. sedula* ARS50-2 increased drastically to the maximum at the 9th day and maintained as the major species since then. *M. sedula copA* mutant was also abundant, but with much lower proportion of the consortium population as compared with that in consortium A.

M. sedula copA mutant in consortium A was still the predominant species throughout the bioleaching process at PD of 3% (w/v) (Fig. 5c). Increased viability of *M. sedula copA* mutant was detected during the first 9 days, thereafter it decreased significantly and remained at low level, which was probably ascribed to the inhibitory effect imposed by the dissolved Cu^{2+} in leachate. The cell density of *M. hakonensis* HO 1-1 increased significantly at the 15th day as compared with that at the 9th day. The proportion of *M. hakonensis* HO 1-1 in consortium A increased steadily since the 15th day, with a high ratio (46.50%) was detected at the 27th day (Fig. 5c). *M. sedula copA* mutant was substituted by *M. sedula* ARS50-2 as a minor species after this cross-resistant strain had been introduced into consortium A when initiating bioleaching at the PD of 3% (w/v) (Fig. 5d). Its abundance decreased further since the 15th day. *M. sedula* ARS50-2 remained as the major species till the 21st day during enargite bioleaching at 3% (w/v). *M. hakonensis* HO 1-1 was almost undetectable during the first 9 days, then its abundance increased significantly after the 15th day to become the predominant species in the consortium at the end of the bioleaching trial (Fig. 5d). This might be ascribed to the reduced sulfur compounds accumulated during enargite bioleaching, which might be not effectively utilized by these *M. sedula* strains, thus provided substrates for the chemolithoautotrophic growth of *M. hakonensis* HO 1-1.

Introduction of cross-resistant *M. sedula* ARS50-2 to the consortium A consolidated the bioleaching capacity probably by modulating the microbial community structure. The total viability of *M. sedula* strains together with *M. hakonensis* HO1-1 in consortium B was higher than that in consortium A since the 15th day at the PD of 1% (w/v), which might confer higher Fe^{2+} and sulfur oxidation capacities and, therefore, led to the slightly higher copper recovery yield (Fig. 3f). With the increase of PD to 3% (w/v), the bioleaching capacity of consortium A was significantly inhibited ascribing to the decrease of viability of *M. sedula copA* mutant imposed by Cu^{2+} , with only 35.28% copper

recovered; however, the bioleaching capacity of consortium B that containing the cross-resistant *M. sedula* ARS50-2 was just slightly inhibited, with 61.57% copper recovery was achieved.

Taken together, the increased Cu^{2+} resistance conferred by mutations that occurred during ALE was critical for *M. sedula* ARS50-2 to decrease the viability of *M. sedula copA* mutant and increase the viability of *M. hakonensis* HO1-1 when co-existing in consortium, especially at elevated pulp density. The data in this study are insightful for the succession of microbial community structure usually observed during the consecutive adaptation or application of bioleaching consortium to process sulfide minerals at high pulp density [26, 39]. Owing to the mutations that occurred during the adaptation/application processes, additional novel strains with new traits (such as higher heavy metal resistance or higher growth rate) could be evolved under these selection pressures that were characteristic of high concentrations of heavy metal/metalloid ions in the bioleaching industry. Consequently, the changing microbial community structure altered the bioleaching capacity of the consortium resulting in a consolidated process.

Conclusion

In this study Cu^{2+} and As^{5+} cross-resistant strains of the extreme thermoacidophile *M. sedula* strains were generated using ALE and mutations conferring As^{5+} resistance were identified. Introduction of the cross-resistant *M. sedula* ARS50-2 to a consortium consisted of *Metallosphaera* spp. modulated the microbial community structure and enhanced the bioleaching of refractory enargite. Differences in viability of the *M. sedula copA* mutant and *M. sedula* ARS50-2 correlated with their copper resistance capacity when co-existing in consortium for enargite bioleaching. This study implied that genetic mutations occurred spontaneously might confer new traits (such as Cu^{2+} resistance) to the evolved strains during bioleaching processes, and therefore modulated the microbial community structure and bioleaching capacity.

Acknowledgements This work was supported by the Department of Energy Joint Genome Institute (DOE-JGI) under the Community Sequencing Program (CSP) (proposal ID 1515, project IDs 1036419, 1036422). And the University of Nebraska Cell Development Facility. This work was also financially supported by the China National Basic Research Program (No. 2010CB630901).

References

1. Ai C, McCarthy S, Eckrich V, Rudrappa D, Qiu G, Blum P (2016) Increased acid resistance of the archaeon, *Metallosphaera sedula*

- by adaptive laboratory evolution. *J Ind Microbiol Biotechnol* 43:1455–1465. doi:10.1007/s10295-016-1812-0
2. Ai CB, McCarthy M, Schackwitz W, Martin J, Lipzen A, Blum P (2015) Complete genome sequences of evolved arsenate-resistant *Metallosphaera sedula* strains. *Genome Announc* 3:e01142-15. doi:10.1128/genomeA.01142-15
 3. Allen MB (1959) Studies with *Cyanidium caldarium*, an anomalously pigmented chlorophyte. *Arch Mikrobiol* 32:270–277
 4. Auernik KS, Maezato Y, Blum PH, Kelly RM (2007) The genome sequence of the metal-mobilizing, extremely thermoacidophilic archaeon *Metallosphaera sedula* provides insights into bioleaching-associated metabolism. *Appl Environ Microbiol* 74:682–692. doi:10.1128/aem.02019-07
 5. Brierley CL, Brierley JA (2013) Progress in bioleaching: part B: applications of microbial processes by the minerals industries. *Appl Microbiol Biotechnol* 97:7543–7552. doi:10.1007/s00253-013-5095-3
 6. Bromfield L, Africa CJ, Harrison STL, van Hille RP (2011) The effect of temperature and culture history on the attachment of *Metallosphaera hakonensis* to mineral sulfides with application to heap bioleaching. *Miner Eng* 24:1157–1165. doi:10.1016/j.mineng.2011.03.019
 7. Deveci H (2002) Effect of solids on viability of acidophilic bacteria. *Miner Eng* 15:1181–1189
 8. Doerrler WT, Sikdar R, Kumar S, Boughner LA (2012) New functions for the ancient DedaA membrane protein family. *J Bacteriol* 195:3–11. doi:10.1128/jb.01006-12
 9. Feng S, Yang H, Wang W (2015) Improved chalcopryrite bioleaching by *Acidithiobacillus* sp. via direct step-wise regulation of microbial community structure. *Bioresour Technol* 192:75–82. doi:10.1016/j.biortech.2015.05.055
 10. Feng S, Yang H, Wang W (2016) Insights to the effects of free cells on community structure of attached cells and chalcopryrite bioleaching during different stages. *Bioresour Technol* 200:186–193. doi:10.1016/j.biortech.2015.09.054
 11. Feng S, Yang H, Zhan X, Wang W (2014) Novel integration strategy for enhancing chalcopryrite bioleaching by *Acidithiobacillus* sp. in a 7-L fermenter. *Bioresour Technol* 161:371–378. doi:10.1016/j.biortech.2014.03.027
 12. Huber Gertrud, Spinnler Carola, Gambacorta Agata, Stetter KO (1989) *Metallosphaera sedula* gen. and sp. nov. represents a new genus of aerobic, metal-mobilizing, thermoacidophilic archaeobacteria. *Syst Appl Microbiol* 12:38–47
 13. Hille RPV, Wyk NV, Harrison STL (eds) (2011) Review of the microbial ecology of BIOX[®] reactors illustrate the dominance of the genus *Ferroplasma* in many commercial reactors. *Biohydrometallurgy: biotech key to unlock minerals resources value*. Central South University Press, Changsha
 14. Kotze AA, Tuffin IM, Deane SM, Rawlings DE (2006) Cloning and characterization of the chromosomal arsenic resistance genes from *Acidithiobacillus caldus* and enhanced arsenic resistance on conjugal transfer of ars genes located on transposon *TnAtcArs*. *Microbiology* 152:3551–3560. doi:10.1099/mic.0.29247-0
 15. Latorre M, Cortés MP, Travisany D, Di Genova A, Budinich M, Reyes-Jara A, Hödar C, González M, Parada P, Bobadilla-Fazzini RA, Cambiazo V, Maass A (2016) The bioleaching potential of a bacterial consortium. *Bioresour Technol* 218:659–666. doi:10.1016/j.biortech.2016.07.012
 16. Lattanzi P, Da Pelo S, Musu E, Atzei D, Elsener B, Fantauzzi M, Rossi A (2008) Enargite oxidation: a review. *Earth Sci Rev* 86:62–88. doi:10.1016/j.earscirev.2007.07.006
 17. Li B, Lin J, Mi S, Lin J (2010) Arsenic resistance operon structure in *Leptospirillum ferriphilum* and proteomic response to arsenic stress. *Bioresour Technol* 101:9811–9814. doi:10.1016/j.biortech.2010.07.043
 18. Maezato Y, Johnson T, McCarthy S, Dana K, Blum P (2012) Metal resistance and lithoautotrophy in the extreme thermoacidophile *Metallosphaera sedula*. *J Bacteriol* 194:6856–6863. doi:10.1128/jb.01413-12
 19. McCarthy S, Ai C, Wheaton G, Tevatia R, Eckrich V, Kelly R, Blum P (2014) Role of an archaeal PitA transporter in the copper and arsenic resistance of *Metallosphaera sedula*, an extreme thermoacidophile. *J Bacteriol* 196:3562–3570. doi:10.1128/jb.01707-14
 20. McCarthy S, Johnson T, Pavlik B, Payne S, Schackwitz W, Martin J, Lipzen A, Keffeler E, Blum P (2015) Expanding the limits of thermoacidophily in the archaeon *Sulfolobus solfataricus* by adaptive evolution. *Appl Environ Microbiol* 82(3):857–867. doi:10.1128/aem.03225-15
 21. Motamedi Ali Shafiee, Cai Sheng-Jian, Streicher Stanley L, Arison Byron H, Miller RR (1996) Characterization of methyltransferase and hydroxylase genes involved in the biosynthesis of the immunosuppressants FK506 and FK520. *J Bacteriol* 178:5243–5248
 22. Okibe N, Johnson DB (2004) Biooxidation of pyrite by defined mixed cultures of moderately thermophilic acidophiles in pH-controlled bioreactors: significance of microbial interactions. *Biotechnol Bioeng* 87:574–583. doi:10.1002/bit.20138
 23. Orell A, Navarro CA, Arancibia R, Mobarec JC, Jerez CA (2010) Life in blue: copper resistance mechanisms of bacteria and Archaea used in industrial biomining of minerals. *Biotechnol Adv* 28:839–848. doi:10.1016/j.biotechadv.2010.07.003
 24. Parada F, Jeffrey MI, Asselin E (2014) Leaching kinetics of enargite in alkaline sodium sulphide solutions. *Hydrometallurgy* 146:48–58. doi:10.1016/j.hydromet.2014.03.003
 25. Plackowski C, Hampton MA, Nguyen AV, Bruckard WJ (2013) Fundamental studies of electrochemically controlled surface oxidation and hydrophobicity of natural enargite. *Langmuir* 29:2371–2386. doi:10.1021/la3043654
 26. Rawlings DE, Johnson DB (2007) The microbiology of biomining: development and optimization of mineral-oxidizing microbial consortia. *Microbiology* 153:315–324. doi:10.1099/mic.0.2006/001206-0
 27. odríguez R, Ballester A, Blázquez ML, González F, Muñoz JA (2003) New information on the chalcopryrite bioleaching mechanism at low and high temperature. *Hydrometallurgy* 71:47–56. doi:10.1016/s0304-386x(03)00173-7
 28. Rudrappa D, White D, Yao AI, Singh R, Pavlik BJ, Blum P, Faciotti MT (2015) Identification of an archaeal mercury regulon by chromatin immunoprecipitation. *Microbiology* 161:2423–2433. doi:10.1099/mic.0.000189
 29. Ruiz MC, Vera MV, Padilla R (2011) Mechanism of enargite pressure leaching in the presence of pyrite. *Hydrometallurgy* 105:290–295. doi:10.1016/j.hydromet.2010.11.002
 30. Sasaki K, Takatsugi K, Ishikura K, Hirajima T (2010) Spectroscopic study on oxidative dissolution of chalcopryrite, enargite and tennantite at different pH values. *Hydrometallurgy* 100:144–151. doi:10.1016/j.hydromet.2009.11.007
 31. Sasaki K, Takatsugi K, Kaneko K, Kozai N, Ohnuki T, Tuovinen OH, Hirajima T (2010) Characterization of secondary arsenic-bearing precipitates formed in the bioleaching of enargite by *Acidithiobacillus ferrooxidans*. *Hydrometallurgy* 104:424–431. doi:10.1016/j.hydromet.2009.12.012
 32. Shiers DW, Ralph DE, Bryan CG, Watling HR (2013) Substrate utilisation by *Acidianus brierleyi*, *Metallosphaera hakonensis* and *Sulfolobus metallicus* in mixed ferrous ion and tetrathionate growth media. *Miner Eng* 48:86–93. doi:10.1016/j.mineng.2012.10.006
 33. Song J, Lin JQ, Gao L, Lin JQ, Qu YB (2008) Modeling and simulation of enargite bioleaching. *Chin J Chem Eng* 16:785–790

34. Stookey LL (1970) Ferrozine-a new spectrophotometric reagent for iron. *Anal Chem* 42:779–781
35. Struck A-W, Thompson ML, Wong LS, Micklefield J (2012) s-Adenosyl-methionine-dependent methyltransferases: highly versatile enzymes in biocatalysis, biosynthesis and other biotechnological applications. *ChemBioChem* 13:2642–2655
36. Sun H, Chen M, Zou L, Shu R, Ruan R (2015) Study of the kinetics of pyrite oxidation under controlled redox potential. *Hydrometallurgy* 155:13–19. doi:[10.1016/j.hydromet.2015.04.003](https://doi.org/10.1016/j.hydromet.2015.04.003)
37. Takatsugi K, Sasaki K, Hirajima T (2011) Mechanism of the enhancement of bioleaching of copper from enargite by thermophilic iron-oxidizing archaea with the concomitant precipitation of arsenic. *Hydrometallurgy* 109:90–96. doi:[10.1016/j.hydromet.2011.05.013](https://doi.org/10.1016/j.hydromet.2011.05.013)
38. Uddin MN, Abdus Salam M, Hossain MA (2013) Spectrophotometric measurement of Cu(DDTC)₂ for the simultaneous determination of zinc and copper. *Chemosphere* 90:366–373. doi:[10.1016/j.chemosphere.2012.07.029](https://doi.org/10.1016/j.chemosphere.2012.07.029)
39. Wang YG, Zeng WM, Qiu GZ, Chen XH, Zhou HB (2014) A moderately thermophilic mixed microbial culture for bioleaching of chalcopyrite concentrate at high pulp density. *Appl Environ Microbiol* 80:741–750
40. Watling H, Shiers D, Collinson D (2015) Extremophiles in mineral sulphide heaps: some bacterial responses to variable temperature, acidity and solution composition. *Microorganisms* 3:364–390. doi:[10.3390/microorganisms3030364](https://doi.org/10.3390/microorganisms3030364)
41. Watling HR, Watkin ELJ, Ralph DE (2010) The resilience and versatility of acidophiles that contribute to the bio-assisted extraction of metals from mineral sulphides. *Environ Technol* 31:915–933. doi:[10.1080/09593331003646646](https://doi.org/10.1080/09593331003646646)
42. R-B Zhang, M-M Wei, H-G Ji, X-H Chen, G-Z Qiu, H-B Zhou (2008) Application of real-time PCR to monitor population dynamics of defined mixed cultures of moderate thermophiles involved in bioleaching of chalcopyrite. *Appl Microbiol Biotechnol* 81:1161–1168. doi:[10.1007/s00253-008-1792-8](https://doi.org/10.1007/s00253-008-1792-8)